Mausam, (1988), 39, 4, 367-374

551.515.5 : 551.524.36

A model of tropical storm from temperature anomaly distributions

J. C. MANDAL

Meteorological Office, New Delhi

(Recieved 29 December 1986)

सार — वास्तविक तूफान में कुछ जाने माने मूल्यों द्वारा अक्ष सममित स्थायी अवस्था के उष्णकटिबंधीय तूफान में तापमान असंगति बंटनों का पता लगाने और इसके द्वारा तूफान के वेग और दाब बंटनों का पता लगाने की विधि के लिए एक सरल समीकरण का संरूपण किया गया है। असंगति क्षेत्र के कल्पित प्रतिरूपी बंटन वाले कुछ मामलों के अध्ययनों का विवेचन किया गया है। इसमें यह पाया गया कि असंगति क्षेत्र के क्षैतिज बंटन के अलावा, इसके उध्वार्धर बंटन पर भी तूफान का सामर्थ्य निर्भर करता है। अधिकतम स्पर्श रेखीय वेग सहित अधिकतम तापमान असंगति से संबधित प्रोफाइलों और न्यूनतम समुद्र दाब को भी प्रयुक्त किया गया है जिसका प्रतिरूपी वास्तविक तूफानों के साथ पूरक संबंध है और नोमोग्राफ के रूप में सरलता से प्रयोग में लाया जा सकता है।

ABSTRACT. A simple equation has been formulated to find out the temperature anomaly distributions in axisymmetric steady state tropical storm from a few known values in the real storm and a method to find out the velocity and pressure distributions of storm from it. A few case studies with assumed typical distribution of anomaly field have been discussed. It has been found that in addition to horizontal distribution of anomaly field, strength of the storm depends on its vertical distribution also. Profiles relating to the maximum temperature anomaly with maximum tangential velocity and that with minimum sea level pressure are also presented which have good agreement with typical real storms and can be readily used as a nomogram.

1. Introduction

Although tropical cyclones vary with respect to size intensity and asymmetry, location, direction of movement etc, there are strong evidences that their basic structures and energetics are similar neglecting the obvious differences between them.

Over ocean areas, the feasible methods for monitoring tropical cyclones are through use of meteorological satellite and aircraft reconnaissance. Numerical methods of storm motion need the wind speed as input ; storm surge models are sensitive to wind speed. The Dvorak technique estimates maximum sustained wind in a tropical cyclone from the shape, size and vertical extent of cloudiness obtained from satellite cloud imageries. However, it yields little or no direct information regarding spatial wind or surface pressure distributions, because they are not well correlated with cloudiness patterns.

From dropsonde, aircraft and micro-wave observations from space, temperature anomalies in and around the storm centre can be estimated with reasonable accuracy. Once the temperature anomalies are known, pressure and tangential wind distribution above the boundary layer can be calculated. Then using boundary layer equations, wind components in the boundary layer can be obtained. Finally using these results, radial and axial velocities for the upper layer can also be found out. But in this process a very large number of temperature data are required which is not practically feasible to get. Therefore, some technique is necessary which can deal with the problem with smaller number of data.

Main objective of this paper is to present a suitable simple mathematical form of the temperature anomaly profile of steady state axisymmetric storm in which it is not necessary to feed the anomaly temperature data at every grid point in the storm and relate the temperature field to tangential velocity and pressure distributions in it. A few standard temperature anomaly profiles have been presented and result from numerical calculations discussed. Finally two profiles, one relating the maximum temperature anomaly with maximum tangential velocity and the other, that with minimum sea level pressure, which have good agreement with real storms have been presented. These can be used readily to determine the strength of the storm.

2. Thermal structure of tropical storm

Numerous case studies of tropical cyclones based on National Hurricane Research Project reconnaissance aircraft data of USA have confirmed that the development of tropical storm is accompanied by intense warming of the upper troposphere. Maximum warming of the order of 10° to 12°C is realistic for minimal hurricane.

Frank (1977) has shown that mean two dimensional temperature anomaly persists through the troposphere. In the boundary layer, temperatures are relatively constant

with radius despite decreasing pressure towards the centre. According to him, maximum temperature anomaly occurs at about 250 mb. Koteswaram (1967) pointed out that hurricane has warm core below 15 km and cold core aloft, highest positive temperature anomaly occurs at 8-12 km.

Simpson (1952) studied typhoon *Marge* (August 1951), its central pressure fell to 895 mb and at a distance of 200 miles from the centre, wind reached full typhoon force (74 miles per hour). Eye soundings revealed exceptionally warm temperature (16° to 18° C warmer) in core region. At 9000 ft eye centre was nearly 8° C warmer than the adjacent area. Hawkins and Imbembo (1976) studied small intense hurricance, *Inez* (1966). It was very small in diameter but at the same time very intense. Maximum wind speed of 157 kt was reported just 12 km from the centre of the eye and hurricane force winds were confined to an area within 66 km from the centre. A maximum temperature anomaly greater than 16°C was located at about 250 km with separate anomaly centre at 600 mb. La Seur and Hawkins (1963) discussed the structure of hurricane *Cleo* (1958). At the higher level temperature gradients were less than those at lower levels. In the lower levels positive anomalies were confined mostly to the eye region and portions of the surrounding wall cloud. They also remarked that gradient wind is a good approximation to the actual wind. Hawkins and Rubsum (1968) studied the hirricane *Hilda* (1964). It was a nearly circular fairly symmetric storm. The strongest horizontal temperature gradients occurred in the eye wall at a level below 550 mb. The centre of warm anomalies (+16° C) was located at 250 mb and a anomaly of about 12° C persisted at 180 mb. Hurricane *Daisy* (1958) was studied by Riehl and Malkus (1961) and others. The positive temperature anomalies associated with the core of the storm were symmetrically distributed with large portion of temperature rise occurring within 25 n. m. of the eye.

3. Basic assumptions

The essential assumptions made in this study is that the vortex is steady and axisymmetric. Though research aircraft missions and synoptic data have demonstrated asymmetries and mesoscale detail of tropical storms, the symmetrical model remains attractive, because of its simplicity and describing some important structural features of certain fully developed storm. The strong surface wind can be traced through the hydrostatic and gradient wind equations to the temperature field with its anomalies in the storm field. The vertical shear of the tangential wind also must be related to the radial temperature gradient. Hawkins and Rubsum (1968) calculated the vertical wind shear for four levels using thermal wind relation assuming gradient balance in steady state frictionless motion from 900 mb wind (real data) at 5 n. m. interval and 100 mb vertical increments. They found that the differences between the calculated data and real data were small and negligible. They remarked that momentary excess of wind over gradient balance may well exist in gust or bubbles (due to liberation of heat in cumulonimbus cloud) and it seems unlikely that over any appreciable time period or any extensive area excessive imbalance can be maintained.

4. Formulation of the problem

The vertical cross-section of temperature anomaly profiles prepared from soundings and aircraft data using mean tropical sounding as normal by La Seur and Hawkins (1963), Hawkins and Rubsum (1968) and Frank (1977) reveal that at lower levels positive anomalies are confined mostly to the eye region and portion of the surrounding wall clouds. Both the magnitude and areal extent of positive anomalies increases upwards with the result that at higher levels one finds positive values within a larger area from the centre. Strongest temperature gradients occur in the eye wall at a level approximately below 550 mb, although the centre of maximum anomaly is located at a higher level. There is a lack of significant positive anomaly below 15,000 ft outside the eye wall. The horizontal gradients above 500 mb level in the outflow layer are much weaker than that through wall clouds at lower level. It is also weaker just near the centre through entire depth of the storm.

Keeping in view the anomaly profiles presented by above authors and other, attempts have been made to find out a suitable analytical expression in terms of vertical height z and radial distance r, from the centre of the storm relating maximum anomaly at the centre, which can represent the anomaly temperature profiles consistent with the observed typical sea level pressure and tangential velocity profile. In formulating the expression, it is assumed that on the sea surface, the anomaly is zero, increases with height becomes maximum at a certain level, then decreases and again becomes zero where the influence of the storm is negligible. On any horizontal plane it is maximum at the centre, decreases rapidly in the wall cloud region, then slowly in the outer region and tends to zero where the influence of the storm is negligible. Using cylindrical coordinates and assuming centre of the storm at $r = 0$, the following expressions for the anomaly temperature field on a r-z plane have been found suitable :

$$K(z)T_{\max} = T_a + \frac{T_a (A_T - T_a)}{T_a + B_T} \times F(r) \quad (1)$$

where, r is a non-dimensional radial distance from the origin, measured on a horizontal plane and z is the non-dimensional height above mean sea level. Reference lengths for non-dimensionalization will be mentioned later on alongwith other variables in Section 4(a).

$K(z)$, is a non-dimensional function of z, which specifies the vertical distribution of temperature anomaly in the centre of the storm such that its values are zero at sea surface and at the top of the storm and has a maximum value of unity where the anomaly is maximum.

$T_{\max}$, is the maximum anomaly at the centre ($r=0$) of the storm.

T_a is the anomaly temperature at any point in the r-z plane.

A_T is a parameter having the dimension of temperature and greater than $T_{\max}$ (*i.e.* $A_T > T_{\max} \geqslant T_a$)

B_T, is a positive parameter with dimension of temperature.

$F(r)$, is a non-dimensional function of r, which specifies the radial anomaly distribution. Its value is zero at $r=0$ and increases rapidly around $r=1.0$, then exponentially. Construction of the function $F(r)$ is discussed in Section 5.

Thus, if in the centre of the storm ($r=0$); where $F(r)$ is equal to zero, the vertical distribution of the temperature anomaly T_a is known, the function $K(z)$ becomes known. At a constant height, left hand side of the Eqn. (1) is constant, so if the radial distribution of the anomaly temperature is known (preferably at the height of maximum anomaly at the centre), the function $F(r)$ also can be calculated from Eqn. (1), with suitable values of the parameter A_T and B_T. However, if radial distribution of T_a is known on more levels, more accurate values can be assigned to these parameters.

Once the functions $K(z)$ and $F(r)$ are thus constructed, the values of T_a at any point in r-z plane can be calculated from the following relation :

$$T_a^2\,[1.0 - F(r)] + T_a\,[B_T + A_T.F(r) - G(z)] - B_T\,G(z) \tag{2}$$

where, $G(z)=K(z).\ T_{max}$

The actual temperature T, in and around the storm is obtained by adding the anomaly temperature T_a to the mean undisturbed temperature $\bar{T}$, which is constant on a horizontal plane, *i.e.*,

$$T=\bar{T}+T_a \tag{3}$$

4 (a). *Method of calculation of tangential velocity and pressure distribution*

In accordance with hydrostatic and gradient balance assumptions to find out the tangential velocity V on r-z plane the following relation can be obtained by eliminating pressure gradient term in gradient wind equation using hydrostatic equation and equation of state :

$$\frac{\partial}{\partial z}\left(\frac{V^2+frV}{r\,T}\right) = -g\,\frac{\partial T}{\partial r}\Big/T^2 \tag{4}$$

where, r is the radial distance, z is the height from the mean sea surface, g is accelaration due to gravity, T is the temperature in °K and f is coriolis parameter.

Similarly pressure distribution p, can be obtained by eliminating density from hydrostatic equation using equation of state in the following form :

$$\frac{1}{p}\frac{\partial p}{\partial z} = -\frac{g}{RT} \tag{5}$$

where, R is the specific gas constant.

The following relations are used to get the non-dimensional form of the variables in Eqns. (1) to (5) :

$$z=Hz' \ ;\ r=r_0r' \ ;\ V=r_0fv \ ;\ g=\frac{(r_0f)^2}{H}\,g'$$

$$p=p_0p' \ ;\ T=T_0T' \ ;\ R=\frac{(r_0f)^2}{T_0}\,R' \tag{6}$$

where, H is the vertical height above which atmosphere is assumed to be undisturbed, r_0 is the approximate inner radial distance of the eye wall cloud, T_0 is sea surface temperature and p_0 is undisturbed sea surface pressure.

Omitting prime and cancelling common factor Eqns. (4) and (5) reduce to the following non-dimensional form :

$$\frac{\partial}{\partial z}\left(\frac{v^2+r\,v}{r\,T}\right) = -\,g\,\frac{\partial T}{\partial r}\Big/T^2 \tag{7}$$

$$\frac{\partial}{\partial z}(\ln p) = -\frac{g}{RT} \tag{8}$$

At $z=1.0$, T is constant radially, so $v=0$. Integrating Eqn. (7) downward from this level w.r.t. z to lower levels and at different radial distance r, the distribution of v in r-z plane can be obtained from the following equation :

$$\left[\frac{v^2+r\,v}{T}\right]_1^z = -\,g\,r\int_1^z\left(\frac{\partial T}{\partial r}\Big/T^2\right)dz \tag{9}$$

Similarly, the pressure distribution p, in the same plane can be claculated integrating in the same way from the same level in the following form :

$$p=p_1\ \exp\left(-\frac{g}{R}\int_1^z\frac{dz}{T}\right) \tag{10}$$

where, p_1 is the pressure at $z=1.0$

To integrate Eqns. (9) and (10), the vertical height z, can be divided into a large number of intervals (say 200 divisions and $\triangle z=h=0.005$) and it can be grouped into sub-divisions comprising five intervals to apply the following more accurate 6 point formula with conventional notation neglecting the remainder R_n which is very small.

$$\int_{z_1}^{z_1+5h} f(z)\,dz = \frac{5h}{288}\Big[\,19f(1)+75f(2)+50f(3)+50f(4)+75f(5)+19f(6)\,\Big]+R_n \tag{11}$$

where, $R_n = -\,\dfrac{275}{12096}\,f^{iv}(\xi)$

5. Results from a few ideal temperature anomaly distributions

For numerical calculation to test the formulation of the problem, the vertical height H, above which the atmosphere is assumed to be undisturbed is taken equal to 16 km, reference radial distance $r_0=50$ km and the non-dimensional radial function $F(r)$ of the following form :

$$F(r) = r^2/(1.0+r^2) + \tfrac{1}{4}\ln(1.0+r^4) \tag{12}$$

The function $F(r)$ has been constituted in such a way that the radial temperature gradient remains small near the centre of the storm, becomes higher in the eye wall region then decreases slowly and becomes insignificant at a large distance from it. It became necessary to express the function as the sum of two functions to specify two different characteristics in inner and outer region of the storm. The influence of the first function on anomaly temperature distribution is important in the inner and eye wall region while that of the second function is in the outer region. Changing the exponents of r, in $F(r)$, variation in radial gradient of anomaly temperature can be made. However, the above expression was found consistent with real storm.

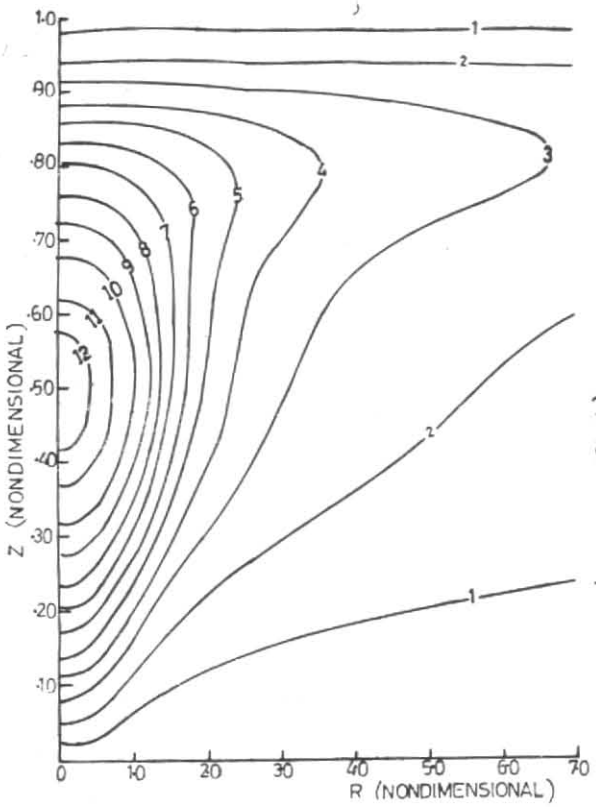

Fig. 1. Temperature anomaly (case 1a) [units °C]

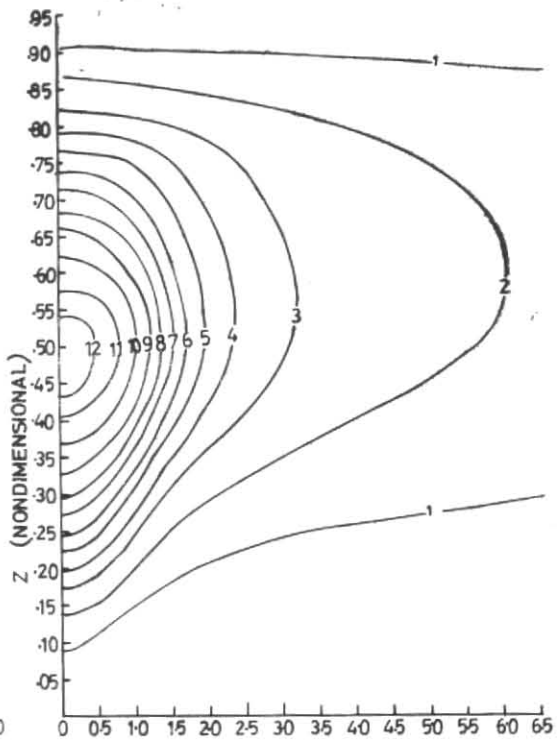

Fig. 2. Temperature anomaly (case 1b) [units °C]

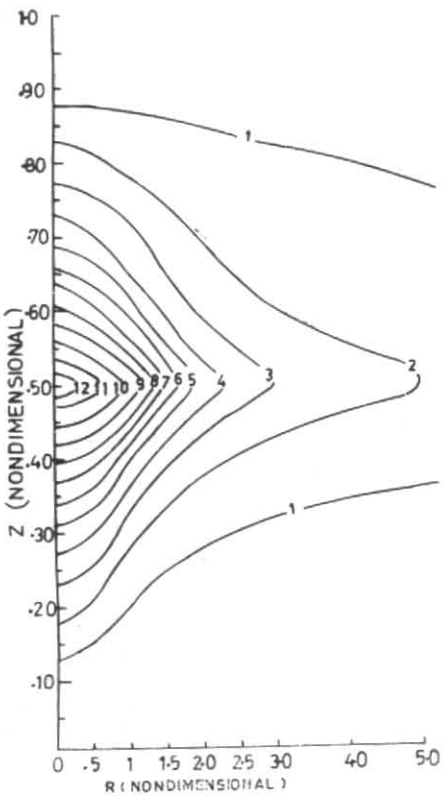

Fig. 3. Temperature anomaly (case 1c) [units °C]

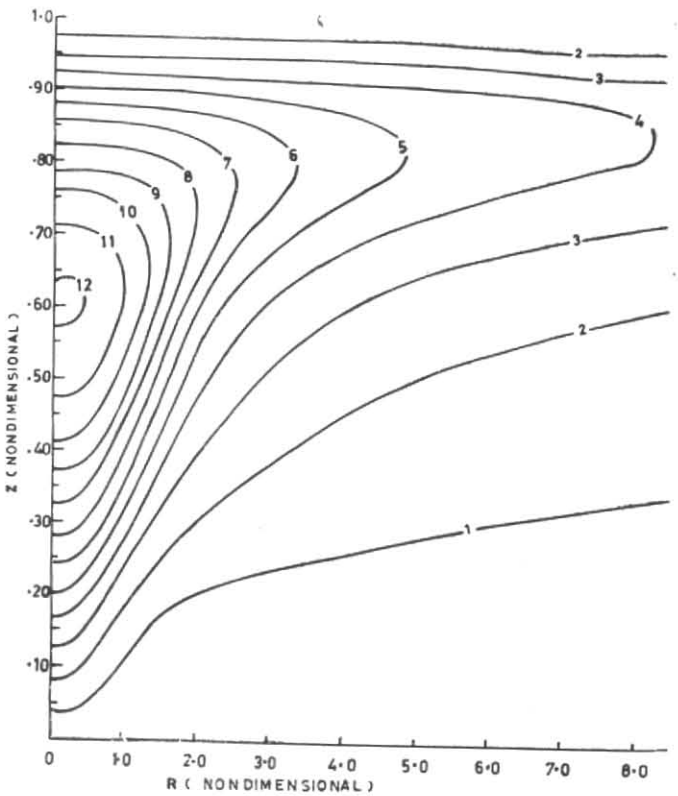

Fig. 4. Temperature anomaly (case 2a) [units °C]

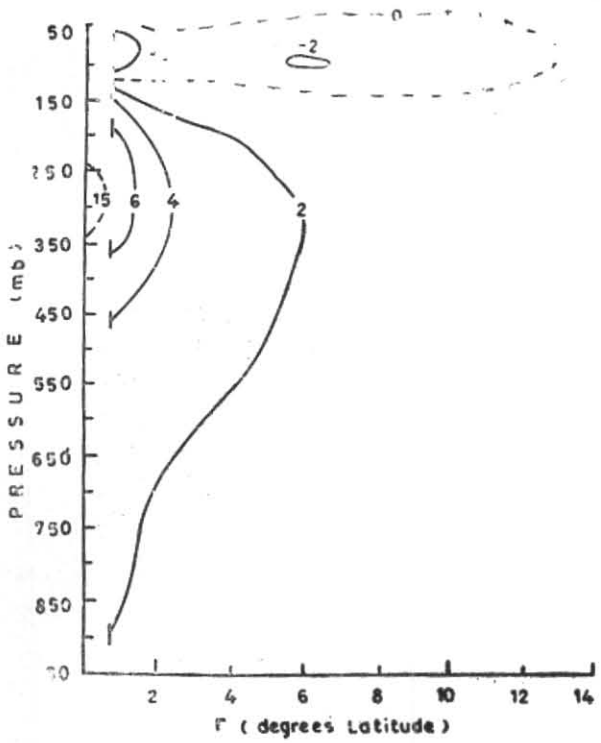

Fig. 5. Temperature anomaly ($T-Tr=14°$) for mean steady state typhoon (unit °C)

Due to the out flow in the upper troposphere, anomaly heat spreads in a larger area and so, radial temperature gradient becomes less there and anomaly profiles bulge outwards. To incorporate this effect, r has been multiplied by the non-dimensional factor $1/(1+z^8)$ and values of the parameters A_T and B_T have been taken in the following form :

$$A_T = T_{max} + 2.0$$

$$B_T = 5.0 + 72.0 \times z^8$$

In order to see the effect of the height of maximum anomaly and its vertical distributions, two sets of funtions for $K(z)$ have been presented in the following forms.

In the first case the maximum anomaly is considered to be at the height of 8.0 km and for its vertical distribution following three non-dimensional fuctions of z for $K(z)$ have been tested :

1(a) $K(z) = \sin(\pi z)$

1(b) $K(z) = \sin^2(\pi z)$

1(c) $K(z) = 1.0 - |\cos(nz)|$

In the second case the centre of maximum anomaly shifted at the height of 9.6 km and for its vertical variation, following two non-dimensional function of z for $K(z)$ have also been tested:

2(a) $K(z) = 1\ 44721 \sin(\pi z).\exp(4.32377\ z - 2.59462)$

2(b) $K(z) = 1.10557\ \sin^2(\pi z)\exp(2.04153\ z - 1.22492)$

In all cases, maximum anomaly, T_{max} has been taken as 12°C.

5 (a). *Discussion of results*

Fig. 5 shows the temperature anomaly ($T-\overline{T}_r=14°$) for mean steady state typhoon from composite studies of of Frank (1977). In Fig. 5 axial coordinate is in unit of pressure and radial coordinate in degree latitude in which the scale is very small. We are not considering negative anomaly at the top, which is probably due to overshooting of the cumulonimbus clouds. It has been pointed out that in composite studies, storms of various dimensions and intensities are averaged together, so it represents a general feature.

Figs. 1-3 represent the anomaly temperatue distributions of cases 1(a), 1(b) and 1(c) and Figs. 4 & 6 of those in cases of 2(a) and 2(b) respectively. The coordinates are in non-dimensional units of length. Figs. 7 & 8 show the comparison of surface tangential velocity and sea level pressure profiles for different vertical distributions and positions of maximum anomaly temperature at the centre of the storm. Fig. 9 represents the surface tangential velocity and sea level pressure profiles in case of 1(c).

When the maximum anomaly temperature is in the middle of the storm's height (*i.e.*, at 8.0 km), but the vertical distributions in the centre ($r=0$) vary, it produces different anomaly temperature profiles (Figs. 1-3). In case of 1(b) (Fig. 2) 1° C anomaly temperature profile starts from a higher level than 1(a) (Fig. 1) and in case of 1(c) (Fig. 3) it is from further higher level. Vertical gradient of anomaly temperature is more in the lower level in case of 1(a), between central and lower part in case of 1(b) and in central parts in case of 1(c), where liberated heat is more concentrated. In case of 1(a) outward profiles in higher level bulge more outwards and radial gradient of anomaly is confined in a narrower zone through larger depth than other two cases, case (c) being least. Comparison of corresponding maximum tengential velocity and fall of central sea level pressure as shown in Figs. 7-9, it is evident that it is maximum in case of 1(a) in which vertical gradient of anomaly is more in lower level and radial gradient is confined in narrow zone through larger depth and minimum in case of 1(c), where vertical gradient is more in central region and larger radial gradient around same radial distance is confined through smaller depth; case 1(b) being in between them.

When the position of maximum anomaly in the centre is shifted upwards at 9.6 km, cases 2(a) (Fig. 1) and 2(b) (Fig. 6), the curvature of the anomaly profiles becomes more prominent, in the lower level it approaches to bell-shaped and 1°C profile shifts upwards; at higher level it bulges more outwards which is more in 2(a) than 2(b). As in cases of 1(a) and 1(b), radial gradient of anomaly temperature in 2(a) is confined in narrow region and greater depth than 2(b) and maximum surface tangential velocity and fall in sea level central pressure, is more in case of 2(a) than 2(b). These two profiles are more representative to the typical real storm.

As shown in Fig. 7, though the maximum fall in central sea level pressure in both the cases 1(a) and 2(a) are nearly same, maximum tangential velocity is more when the maximum anomaly is at 8.0 km than that at 9.6 km. This is due to the fact that the pressure profile in the former case is steeper in the eye wall region than the latter case. In case of 1(b) and 2(b) (Fig. 8) maximum fall in central pressure is slightly

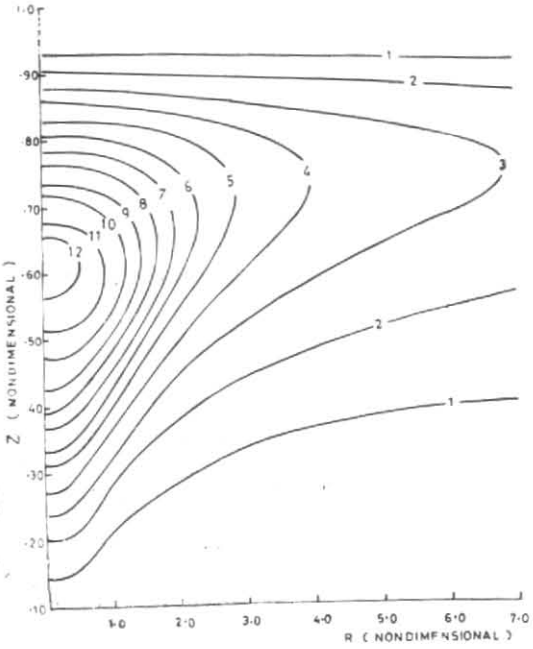

Fig. 6. Temperature anomaly (case 2b) [units °C]

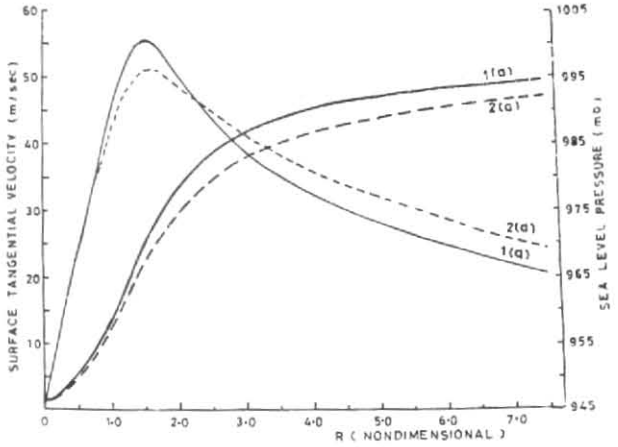

Fig. 7. Surface tangential velocity and sea level pressure, $T_{max} = 12°C$

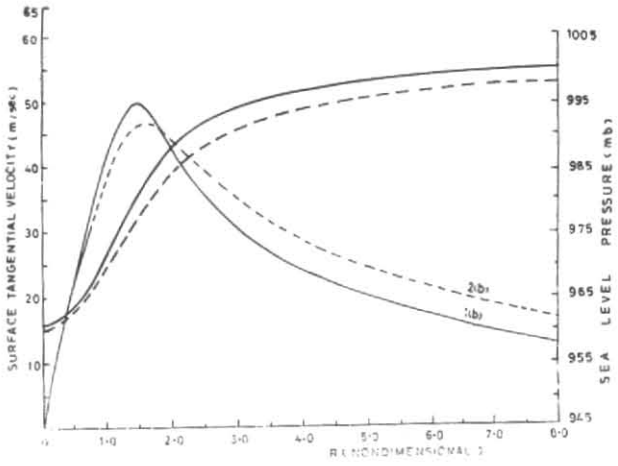

Fig. 8. Surface tangential velocity and sea level pressure, $T_{max} = 12°C$

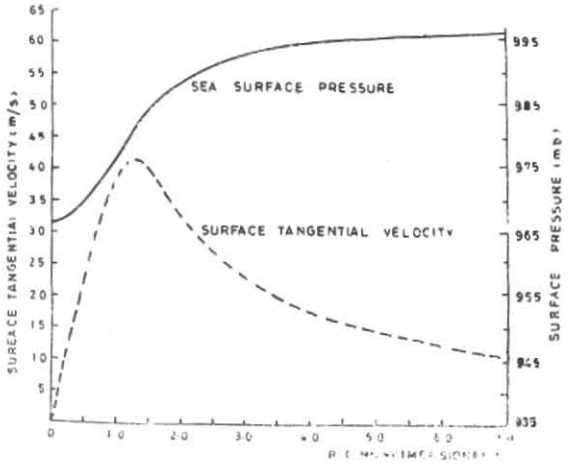

Fig. 9. Surface tangential velocity and sea level pressure, $T_{max} = 12°C$

less when the maximum anomaly is at 8.0 km than that at 9.6 km but the maximum sea surface tangential velocity is more when maximum anomaly is at 8.0 km which is due to the steeper pressure profile than the other in the eye wall region. When maximum anomaly is shifted at higher level, sea surface tangential velocity in the outer region becomes more than that a lower level. This is due to more outwards spreading of the anomaly profile at higher level.

Vertical cross-section of the tangential velocity, relative vorticity and absolute angular momentum in case of 2(b) in r - z plane have been calculated and found to be similar to the composite studies. It is evident from Figs. 1 and 6 that the horizontal gradient of temperature is less in upper level and its contribution to the increase of pressure gradient is less. It is due to the fact that in higher levels liberated heat cannot remain concentrated in the central region due to outflow. In

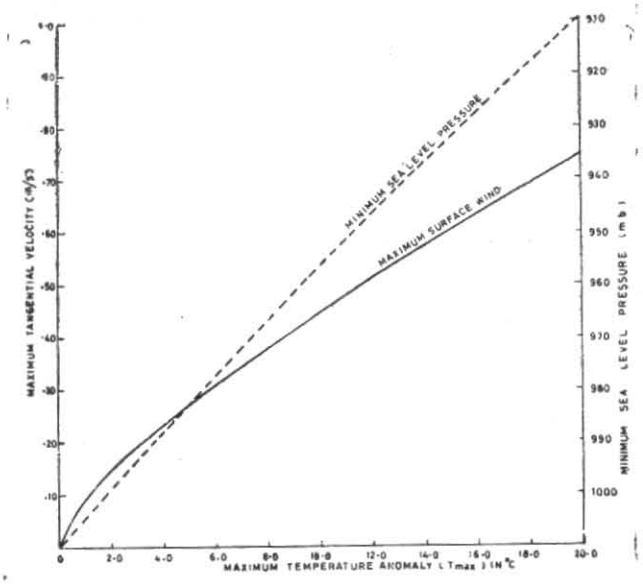

Fig. 10. Maximum temperature anomaly *versus* maximum tangential velocity and minimum sea level pressure

TABLE 1

Storm (yr)	Observations			Calculation		
	Max. surface wind (m/sec)	Min. sea level pressure (mb)	Max. Temp. anomaly (°C)	Max. surface wind (m/sec)	Min. sea level press. (mb)	Remarks
Dora (1964)	41	—	10	45		
Cleo (1958)	46	—	11	48		
Hilda (1964)	56	—	15	60		
Daisy (1958)	43	—	8.5	40		At 620 mb
Inez (1966)	79	—	More than 16	72 75		Taking 19° C ,, 20° C
Phyllis (1975)	61	925	—		931	
Betty (1975)	49	947	—		951	
Cora (1975)	53	943	—		943	
Tess (1975)	49	945	—		950	
Alice (1975)	38	973	—		968	

this study as the radial function $F(r)$ has been specified in non-dimensional form, there will be no variation in anomaly curve pattern with variation of the reference radial length r_0. Test computations have been performed with variable r_0 and it was found that there is a slight increase of tangential velocity with decrease of r_0, due to less effect of coriolis term in gradient balance near the centre.

In order to see, how the maximum tangential velocity (v_{max}) and minimum sea level pressure (p_{min}) vary with the variation of maximum temperature anomaly (T_{max}), computations have been done varying T_{max} from 1°C to 20°C with maximum anomaly at 9.6 km with the same radial function $F(r)$ and vertical function $K(z)$ as in case 2(a). The v_{max} curve and p_{min} curve against T_{max} are shown in Fig. 10. If any one of the three variables, is known other two can be found out from the graph. For pressure curve, the undisturbed sea level pressure has been taken as 1010 mb. The gradient of pressure curve is slightly higher at lower T_{max} than higher. In the maximum velocity curve also the gradient gradually decreases from lower value of T_{max} to its higher values. Variation is more prominent in lower values. Table 1 shows the comparison of the available real data that with the values represented in Fig. 10. The real data have been taken from different published papers. Though the number of real data is small, it shows good agreement with the computed values. If only the maximum anomaly at the centre of storm is known a good estimate with reasonable accuracy of the minimum sea level pressure of typical cases can be made from the curve of Fig. 10, without going in detail calculations of anomaly

distributions in space. Moreover, if radius of maximum wind can be estimated from cloud pattern, the tangential velocity and pressure distribution in r-z plane can be estimated with the function $F(r)$ and $K(z)$ used in calculations of Fig. 10.

6. Conclusions

The method presented in this work is simple and easy to apply. If the anomaly distribution in the centre and in radial direction at least at one level through the maximum anomaly are known, the results will be more accurate. The graphs presented in Fig. 10 are still simpler. This is a preliminary attempt, and if more real data are available, case 2(a) (Fig. 10) can be further modified with variation of parameters used in the original equations.

Acknowledgements

The author expresses his deep gratitude to Dr. Ambarish Ghosh, Professor, Indian Statistical Institute and Calcutta University, Department of Applied Mathematics, who inspired for this study, gave valuable suggestions and provided computer facilities in ISI during preliminary test of the problem. Final computation has been done in IMD, NHAC, Computer Centre, New Delhi. The author wishes to express his thanks to Shri D.K. Mishra, Director, Sat. Met. Directorate, who has kindly gone through the manuscript and expressed his views.

References

Frank, W.M., 1977, "The structure and energetics of the tropical cyclone, I: Storm Structure", *Mon. Weath. Rev.*, **105**, pp. 1119-1135.

Hawkins, H.F. and Imbembo, S.M., 1976, "The structure of a small intense hurricane—Inez 1966", *Mon. Weath. Rev.*, **104**, pp. 418-422.

Hawkins, H.F. and Rubsum, D.T., 1968, "Hurricane Hilda 1964, Structure and budgets of hurricane in October 1, 1964", *Mon. Weath. Rev.*, **96**, pp. 617-636.

Koteswaram, P., 1967, "Upper tropospheric and lower stratospheric structure of several hurricanes", NHR-Technical Memo. No. 79.

La Seur, N.F. and Hawkins, H.F., 1963, "An analysis of hurricane Cleo (1958) based on data from research reconnaissance aircraft", *Mon. Weath. Rev.*, **91**, pp. 694-709.

Riehl, H. and Malkus, J.S., 1961, "Some aspects of hurricane Daisy (1958)", *Tellus*, **13**, pp. 181-213.

Simpson, R.H., 1952, "Exploring the eye of typhoon Marge (1951)", *Bull. Amer. met. Soc.*, **33**, pp. 286-298.